MULTIPLE REFLECTION EFFECTS DURING THE IN-SITU CALIBRATION OF AN EMISSIVITY INDEPENDENT RADIATION THERMOMETER

Benjamin J. Brosilow[1], Yoram Naor[1], and Yael Baharav[2]

[1]C. I. Systems, P.O.B. 147, Migdal Ha'emek 10551, Israel
[2]C. I. Systems, 251 Scripps Ct., Palo Alto CA 94306, USA

ABSTRACT

We present an improved in-situ calibration procedure for the reflectometer channel of an integrated radiometer/reflectometer used for emissivity-independent wafer temperature measurement in semiconductor production lines in RTP and other single-wafer processes (HDP-CVD, PVD, etc.). The improved calibration procedure, which has been implemented in our NTM line of radiation thermometers, allows for more accurate wafer temperature measurement, particularly for very low emissivity wafers. The calibration procedure is improved by explicitly accounting for the localized drop in reflectivity of a calibration standard used for the reflectometer calibration, when this standard is brought in close proximity to the radiometer/reflectometer probe tip. The reflectivity of the standard decreases near the probe tip due to a small "cavity effect" interaction between the probe tip and the reflectivity standard. Failure to account for the decreased reflectivity of the calibration standard results in a small reflectometer calibration error, which causes the combined radiometer/reflectometer to exhibit a small residual emissivity dependence in the temperature measurement. The improved calibration procedure eliminates this small emissivity dependence, thus allowing improved temperature measurement accuracy, particularly for high reflectivity (low emissivity) wafers.

INTRODUCTION

Accurate, non-contact, emissivity independent measurement of substrate temperature during semiconductor processing can be achieved by the simultaneous measurement of the substrate radiometric emission and reflectivity within a spectral band at which the substrate is opaque. The temperature is calculated from the target self-emission (E) and reflectivity (ρ) measurements as:

$$\varepsilon = 1 - \rho, \quad \text{(transmission = 0)} \qquad (1)$$

$$E = \varepsilon P(T) \qquad (2)$$

where ε is the target emissivity, and P is the Plank function evaluated at the target temperature T and integrated over the spectral response of the radiometer. Simultaneous, real time measurement of both the substrate self-emission and reflectivity is necessary in semiconductor processing applications because the heating and thin film growth which occur during semiconductor processing can significantly alter the emissivity of the substrate. For example, Fig. 1 shows the change in emissivity measured for a silicon wafer with polycrystalline-silicon on silicon-dioxide thin film layers, as the wafer is heated from 700 to 950°C. Fig. 2 shows a theoretical calculation of the normal reflectivity spectra for a silicon wafer with 100Å amorphous-silicon on 1000Å silicon-dioxide film stack, and the reflectivity spectrum for this same wafer after the deposition

of an additional 400Å of amorphous silicon [1,2]. The growth of the additional 400Å of amorphous-silicon causes a change in normal reflectivity from nearly zero to about 0.7 for measurement wavelengths between 0.9 and 1 μm.

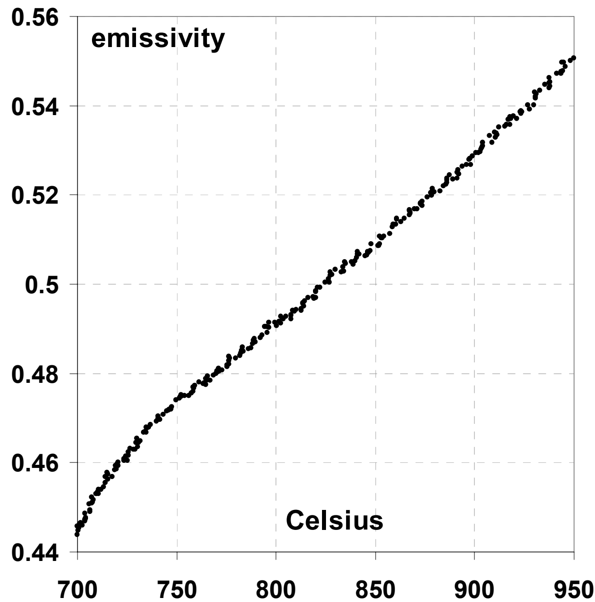

Fig. 1: Experimentally measured emissivity (=1-reflectivity) of a silicon wafer with a poly-silicon on silicon-dioxide thin film stack, as the wafer is heated from 700 to 950°C.

In this paper we discuss issues which arise when performing periodic calibrations of the reflectivity channel of an industrial radiometer / reflectometer used for temperature measurement of substrates during semiconductor processing. Such periodic calibrations are typically performed as part of periodic maintenance of the process reactor to compensate for small changes in the system operation with time-on-line, due to wear and/or deposition on the radiometer / reflectometer optical interface, etc. An important aspect of these periodic calibrations is to eliminate offsets between different thermometers in a single chamber which may measure the temperature at different points on the wafer surface, and to eliminate offsets between different, but nominally "identical" wafer processing chambers, which will be used to run identical wafer processing recipes [3,4,5,6].

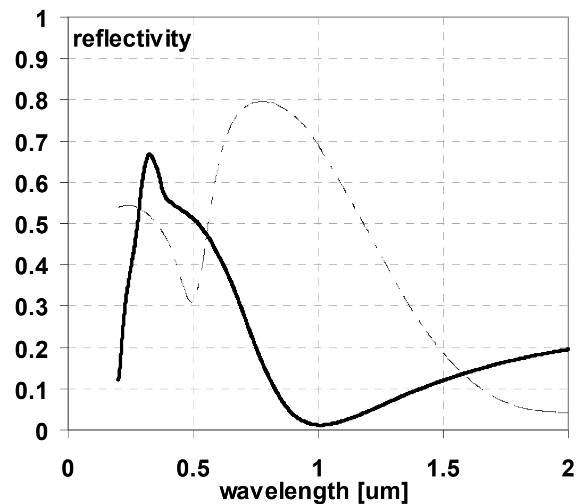

Fig. 2: Calculated normal reflectivity for 100Å amorphous-silicon on 1000Å silicon-dioxide on a silicon substrate (solid curve), and the same film stack after deposition of an additional 400Å of amorphous-silicon (broken curve). The addition of the 400Å of amorphous silicon changes the reflectivity from near 0 to about 0.7 for measurement wavelengths between 0.9 and 1μm.

OPERATION OF THE REFLECTOMETER CHANNEL

The combined radiometer / reflectometer used for this study was the C I Systems NTM500 thermometer [7, 8]. The reflectometer channel of this thermometer operates by sending periodic pulses of radiation out the end of the probe, and measuring the number of photons from these pulses which reenter the probe after reflection off the target surface. An in-situ calibration procedure is used to determine the proportionality constant between the target surface reflectivity and the number of emitted

pulse photons reentering the probe of the installed radiometer / reflectometer:

$$\rho = \frac{\rho_{cal}}{V_{cal}} V \qquad (3)$$

where V is the number of pulse photons which reenter the probe after reflection off the target of reflectivity ρ, and V_{cal} is this number when viewing a calibration standard of reflectivity ρ_{cal}. The factor ρ_{cal} / V_{cal} is determined in-situ by placing a target of known reflectivity ρ_{cal} in the reactor, and measuring the reflectometer response V_{cal}. For example, the "target of known reflectivity" is frequently a polished silicon wafer at room-temperature, with free-space reflectivity 0.319 [9].

When the value ρ_{cal} / V_{cal} is precisely determined, the combined radiometer / reflectometer probe can in principle provide completely emissivity independent temperature measurements via (1) and (2). In practice, a small uncertainty in the value of this calibration constant results in a residual level of emissivity dependence in the measurement. Although this residual emissivity dependence results in temperature errors which are orders of magnitude smaller than the errors produced by non-emissivity compensated pyrometry, it is of course still desirable to minimize such errors to the maximum extent possible. Fig. 3 shows the temperature calculation errors resulting from the residual emissivity dependence when the reflectometer calibration factor ρ_{cal} / V_{cal} is over-estimated by a given amount, for a 700ºC wafer with various emissivities. This figure demonstrates that errors in the reflectometer calibration factor are most significant when measuring targets of low emissivity. In the following sections we discuss a main source of error in the determination of this calibration constant, which occurs when the thermometer probe is placed in close proximity to the wafer during calibration. We then present a method to significantly improve the calibration accuracy in such cases.

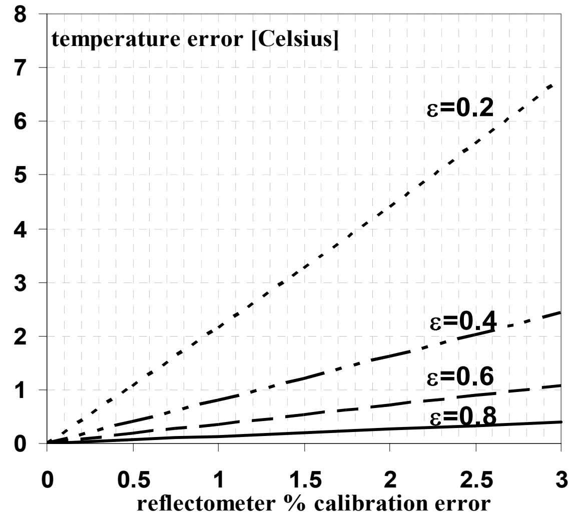

Fig. 3: Temperature error which results when using (1) and (2) to calculate the wafer temperature, while the reflectometer calibration factor ρ_{cal} / V_{cal} of (3) is over-estimated by an amount listed on the abscissa. The four curves correspond, from top to bottom, to 700°C wafers with emissivity 0.2, 0.4, 0.6, and 0.8 respectively.

EFFECT OF PROBE PROXIMITY ON TARGET REFLECTIVITY

A main source of error in the determination of the calibration constant ρ_{cal}/V_{cal} in (3) is failure to account for the localized decrease in reflectivity ρ_{cal} of the calibration standard when the standard is placed in-situ in the reactor with the probe surface in close proximity to the wafer. Since it is usually the free-space reflectivity of this calibration standard which is known, it is necessary to correct this free-space reflectivity value to account for the decrease in reflectivity which occurs when the standard is placed close to the probe surface for the measurement of the reflectometer response V_{cal}. Fig. 4 shows the decrease in reflectivity of surfaces of various free-space reflectivities, as the surfaces approach the probe surface. When the probe-to-target distance is on the order of the probe diameter, a small "cavity effect" develops between the probe-tip and the target surface, resulting in a localized change in both the reflectivity and emissivity of the target surface. In particular, the localized reflectivity is seen to

drop, and consequently, the localized target emissivity increases in such a way that both the fundamental equations (1) and (2) remain valid. Note that the degree of the reflectivity drop is a function of the target free-space reflectivity: the drop is strongest for targets with free-space reflectivities near ~1/2, while no drop is detected for targets with very high reflectivity. The data in Fig. 4 was collected using an NTM500 reflectometer / radiometer probe terminating in a polished quartz rod of diameter 4mm.

We model the measured reflectivity drop shown in Fig. 4 by considering multiple reflections between the thermometer probe-tip and the target surface:

$$V = V_0[\rho_s \eta(1-\rho_p) + (\rho_s \eta)^2 \rho_p (1-\rho_p) + (\rho_s \eta)^3 \rho_p^2 (1-\rho_p) + \ldots] \quad (4)$$

Here V is the number of pulse photons which reenter the probe after reflection(s) off the target surface, V_0 is the number of photons emitted by the probe, ρ_s is the free-space reflectivity of the target surface, η is the fraction of reflected photons which are incident on the probe tip after a single reflection from the target surface, and ρ_p is the free-space reflectivity of the thermometer probe. The first term in (4) accounts for photons entering the thermometer probe after a single reflection off the target surface, the second term for photons entering the probe after two reflections off the target surface (and one reflection off the probe tip), and so on. The factor η accounts primarily for the effect of divergence of the radiation beam emitted by the probe. The divergence of this beam causes the reflected radiation to be spread over an area larger than the probe cross-section, and thus only a fraction of the reflected photons are incident on the probe. Evaluating the infinite sum in (4) gives:

$$V = \frac{m\rho_s}{1 - F\rho_s} \quad (5)$$

where m=$V_0(1\text{-}\rho_p)\eta$, and F=$\rho_p\eta$. This result is the same as the result of the well known infinite parallel plate model [10, 11, 12], where the reflectivity of one of the "infinite plates" is replaced by the effective probe reflectivity $\rho_p\eta$. While this model is an extreme simplification of the actual probe-to-target interaction, it does describe central elements of this interaction.

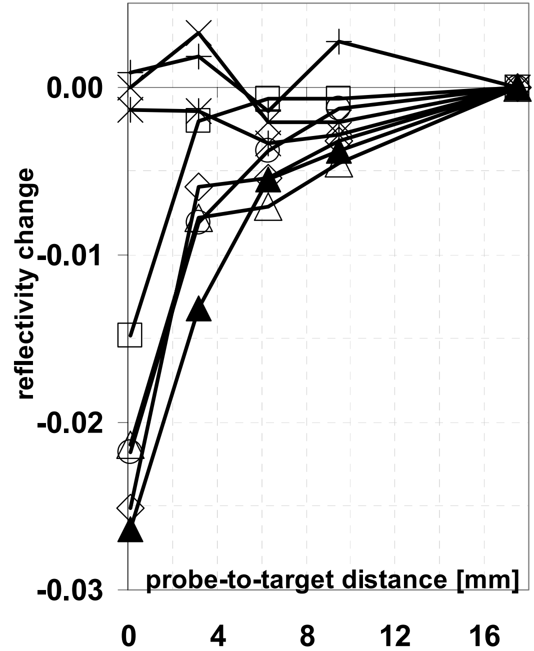

Fig. 4: Measured reflectivity change of various target surfaces as a function of probe-to-target distance: brush polished graphite (□), polished silicon (○), polished germanium (▲), titanium-nitride on polished silicon (◊), cobalt silicide (Δ), aluminum on polished silicon (*), alloy of 3 metals on polished silicon (x), and a Gold mirror (+).

In order to verify the model (5), we used the measured reflectivity signal V from two surfaces of known reflectivity (silver mirror reflectivity = 0.982 and polished silicon reflectivity = 0.319) to solve for the model constants F and m at each probe-to-target distance. Then we plot the free-space reflectivity ρ_s of other target surfaces, calculated based on the reflectivity measurements made at each probe-to-target distance. If the model is valid, we expect the

calculated free-space reflectivity of each target should be independent of the probe position at which the data was collected. Fig. 5 shows that the calculated free-space reflectivity of the various surfaces changes by only 0.5% as the probe approaches the target surface. This small measured change in reflectivity indicates the magnitude of residual phenomenon not accounted for by the model.

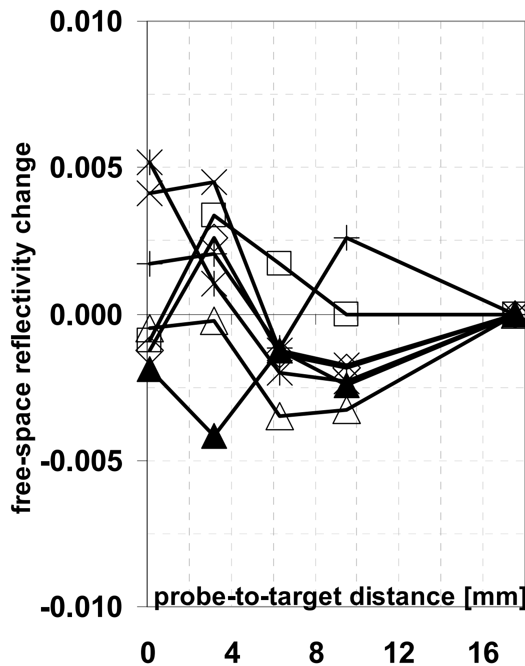

Fig. 5: Change in calculated free-space reflectivity ρ_s for each target surface, according to the model of equation 5. The relative insensitivity of ρ_s to probe-to-target distance compared to the in-situ reflectivity shown in Fig. 4, demonstrates the qualitative validity of the model. Symbols have same meaning as Fig 4.

Fig. 6 shows the value of the constant F calculated from the model (5) based on the reflectivity measurements from the silicon wafer and silver mirror at each probe-to-target distance. At probe-to-target contact, we expect that F will equal the probe reflectivity ρ_p since beam spreading is negligible in this case, and hence the factor η approaches 1 (and $F=\rho_p\eta \approx\rho_p$). Thus we estimate that the probe used in this study has reflectivity 0.152. The probe tip is a quartz-rod light-pipe with ~10% reflectivity, and it follows that the additional 5% reflectivity of the probe comes from reflections off of other thermometer components through which the collected radiation passes, such as a fiber bundle, etc. Even at relatively large probe-to-target distances, F maintains a non-zero value. This may stem from multiple reflections off the surrounding reactor surfaces. In our experimental set-up, the "reactor walls" were constructed from paper with reflectivity 4.3% at the thermometer wavelength.

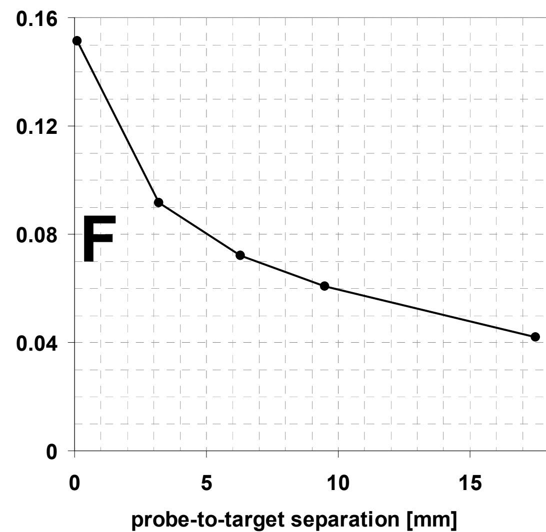

Fig. 6: Model parameter F from (5) as a function of probe-to-target distance

Figure 7 shows the decrease in target reflectivity (compared to the free-space reflectivity) as a function of target free-space reflectivity and probe proximity, as fit to model (5) using the data from the silver mirror and silicon wafer targets. The model predicts that the reflectivity decrease is strongest for targets with reflectivity slightly above 1/2. Indeed, this is demonstrated in the data of Fig. 4 as well, where the reflectivity drop is strongest for the samples with moderate levels of reflectivity. Similarly, Figure 7 shows that targets with reflectivity near 0 or 1 are not strongly effected by the probe proximity, and indeed, the targets in Fig. 4 with reflectivity >0.9 (gold, 3-metal

alloy, and aluminum) show negligible drop in reflectivity due to probe proximity.

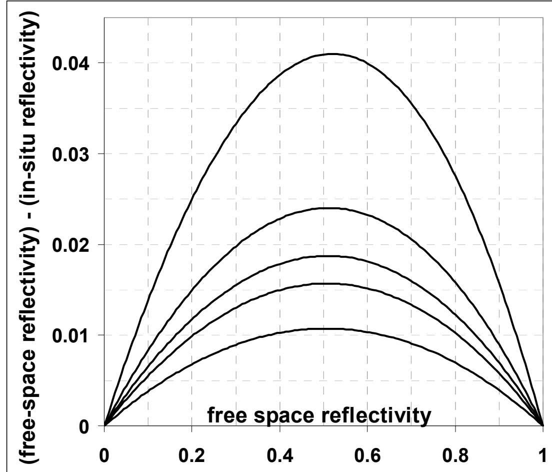

Fig. 7: Reflectivity decrease due to probe proximity, according to model (5), as fit to reflectivity data from a silicon wafer and silver mirror. Curves correspond, from top to bottom, to probe-to-target separation of 0.1, 3.2, 6.3, 9.5 and 17.5 mm.

IMPROVED REFLECTOMETER CALIBRATION PROCEDURE

Equations (1) and (2) are valid for the in-situ values of the reflectivity ρ and emission E. Thus the reflectivity decrease when the probe approaches the target surface does not effect the temperature calculation using these equations. However, one situation where this reflectivity drop does need to be carefully considered is when using standards of known reflectivity to calibrate the reflectometer. In this case, it is the free-space reflectivity ρ_s that is usually known, and the in-situ reflectivity ρ_{cal} required by the calibration equation (3) will be smaller than ρ_s by an unknown amount.

One way to circumvent this in-situ reflectivity drop during the calibration procedure is to calibrate against a reflectivity standard with reflectivity very near 1. Such a highly reflective surface will not be strongly effected by the proximity of the probe tip (figure 7). A more convenient variant of this approach is to initially calibrate the reflectometer using a highly reflective standard, and then use the calibrated system to measure the in-situ reflectivity of a bare silicon wafer (or other convenient standard). Following this initial calibration, all subsequent calibrations can be performed using a bare silicon wafer, and the value of ρ_{cal} for use in the calibration equation (3) will be the in-situ reflectivity of the silicon wafer measured after the initial calibration against the highly reflective standard. The in-situ reflectivity of silicon can be remeasured periodically (against the high reflectivity standard) to account for slow degradation of the system with time-on-line.

Still another possibility for improving the accuracy of the reflectivity channel calibration is to use two reflectivity standards of known free space reflectivity ρ_s to solve for the model constants F and m. These constants calibrate the system according to (3) with $\rho_{cal}/V_{cal} = (1\text{-}F)/m$.

We note that improved calibration accuracy can also be achieved by increasing the probe-to-target distance, which decreases the effect of the probe tip on the reflectivity of the calibration standard. However, operating the thermometer at a large probe-to-target distance has other disadvantages. In particular, equation (1) and (2) are theoretically exactly accurate for reflectivity measured under hemispherical illumination. In practice the reflectometer channel illuminates the target at an angular distribution biased towards normal incidence, and the degree of bias increases as the probe-to-target distance increases. The net effect of this angular bias is that at large probe-to-target distances, the thermometer shows a degree of sensitivity to target roughness (or more generally, sensitivity to changes in the bi-directional-reflectivity-function of the target), in the sense that the temperature measurement is accurate for samples of roughness similar to the roughness of the reflectivity standard, but errors are introduced when the target roughness deviates significantly from that of the reflectivity standard. Placing the probe close to the target surface significantly mitigates such roughness sensitivity by ensuring a more nearly hemispherical illumination of the target.

CONCLUSION

We have developed methods for improving the calibration accuracy of the reflectometer channel of a combined radiometer/reflectometer probe, by accounting for the localized decrease in reflectivity of the calibration standard near the probe tip. The data in Fig. 4 and 5 demonstrates that even the simple "infinite parallel plate" model is sufficient to describe the probe-to-calibration standard "cavity effect" interaction, as long as the reflectivity of the probe is replaced by an "effective reflectivity". By correcting the reflectivity of the calibration standard to account for the reflectivity drop near the probe surface, we improve the accuracy of the reflectometer calibration, and hence improve the combined radiometer / reflectometer temperature measurement accuracy, particularly when measuring low emissivity wafers.

REFERENCES

[1] D. L. Windt Computers in Physics **12** 360-370 (1998).

[2] B J. Lee and Z.M. Zhang, in 11th IEEE International Conference on Advanced Thermal Processing of Semiconductors-RTP2003, IEEE, Electron Devices Society, p. 143 (2003).

[3] K. S. Ball, K. S. Huston, B. L. Noska,, M. A. Simonich, F. T. Geyling, D. Sing, R. S. Tichy and Y. Baharav, Proceedings of the 9th International Conference on Advanced Thermal Processing of Semiconductors, RTP 2001, Editors: D.P. DeWitt, J. Gelpey, B. Lojek, Z. Nenyei. September 25-29, 2001 Anchorage, Alaska. pages 149-162.

[4] W.A. Kimes, K.G. Kreider, D.C. Ripple, B.K.Tsai, in 12th IEEE International Conference on Advanced Thermal Processing of Semiconductors-RTP20043, IEEE, Electron Devices Society, p. 156 (2004).

[5] A. Hunter, B. Adams, A. Rubinchik, G. Pham, 9th International Conference on Advanced Thermal Processing of Semiconductors- RTP2001, p. 169 (2001).

[6] A. Hunter, B. Adams, R. Ramanujam, , in 11th IEEE International Conference on Advanced Thermal Processing of Semiconductors- RTP2003, IEEE, Electron Devices Society, p. 85 (2003).

[7] Yael Baharav, Yaron Ish-Shalom, Graham Jackson, in *ASEAN: Semiconductor Manufacturing Technology*, E. Cooper and L. Davenport eds. (1998).

[8] US patent 6299346 (2001).

[9] P.J. Timans, NATO ASI series E, **318**, p. 35-101 (1996).

[10] D.P. DeWitt, F.Y. Sorrel, and J.K. Elliott, *Mat. Res. Soc. Symp. Proc.*, 470:3 (1997).

[11] F. Rosa, Y.H. Zhou, Z.M. Zhang, D.P. DeWitt, and B.K. Tsai, in *Advanced in Rapid Thermal Processing*, F. Roozeboom, J.C. Gelpey, M.C. Öztürk, and J. Nakos, eds, The Electrochemical Society, Pennington, Proc. Vol. 99-10, pp. 419-426 (1999).

[12] B. Peuse, G. Miner, M. Yam, and C. Elia, "Advances in RTP temperature measurement and control," Mat. Res. Soc. Symp. Proc. **525**, 71 (1998).